

# Effects of UV Radiation and Isothermal Crystallization on LDPE/MMT Nanocomposites

Samir Al-Zobaidi

Department of Physics, College of Science, Majmaah University, Al-Zulfi, 11932, Saudi Arabia, [s.alzobaidi@mu.edu.sa](mailto:s.alzobaidi@mu.edu.sa)

## Abstract

In order to understand the effect of both UV radiation and isothermal crystallization temperature on LDPE/MMT nanocomposites we used one composition of LDPE/MMT nanocomposites. All samples were crystallized isothermally at two selected temperatures of 100 and 104°C for a fixed time of 5h. The crystallization temperature was chosen to be above the non-isothermal crystallization of LDPE/MMT nanocomposites. XRD showed that the material used consisted of two stable monoclinic and orthorhombic phases. Both phases have shown different respond to the crystallization process. Intercalation of clay was also affected by the crystallization temperatures and UV exposure. Results obtained from XRD, DSC and FTIR were in agreement with each other. A third phase that is thermally less stable was also observed, its thermal respond was larger since it contains low molecular weight entities which makes it more vulnerable to any UV exposure.

Keywords: LDPE; montmorillonite; isothermal, crystallization; UV irradiation, nanocomposites.

Article history: Received: July 12, 2015, Accepted: January 26, 2016

## 1. Introduction:

The most common layered silicates used in preparing polymer/layered silicate nanocomposites are Montmorillonite (MMT). It is one of the typical natural minerals in the smectite clay family. The stacked layers of MMT are of about 1 nm in thickness and are separated from each other by a weak dipolar force. They form interlayers or galleries that are usually occupied by exchangeable  $\text{Na}^+$ ,  $\text{K}^+$ ,  $\text{Ca}^{+2}$  and  $\text{Mg}^{+2}$  cations. In order to improve the ion exchangeability of the layered silicates, MMT is usually modified organically by exchanging the alkali counter ions with cationic-organic surfactans, such as alkylammoniums [1, 2].

The organic modification of MMT allows the polymer molecules to intercalate within the galleries. Depending on the strength of the interfacial interactions between the polymer matrix and layered silicates, polymer/layered silicate can form either intercalated nanocomposites, where few molecular layers of

polymer are intercalated, or exfoliated nanocomposites where the individual clay layers are separated in a continuous polymer matrix by an average distances that depends on the clay loadings [3]. Well exfoliated nano-composites show better mechanical properties compared to its pure polymer. However, the interfacial interaction between LDPE and MMT is generally weak and require an intermediate agent like Maleic anhydride.

The importance of LDPE in the different fields of industry is well-known. Based on recent statistics [4], 17.5% of the total consumption of plastic industries in Europe is of LDPE. Its applications vary from food packaging and shopping bags to electrical applications, auto parts, construction sites, and many other important and crucial applications. LDPE/layered silicates composites have shown improvement in their mechanical properties, flame retarding and thermal stability.

The isothermal crystallization of LDPE and some of its blends was studied thoroughly in literature [5-10]. Effect of radiation on the properties of LDPE and LDPE/MMT nanocomposites has also been extensively studied in literature. High energy ion beam irradiation [11-13],  $\gamma$  radiation [14-16] and electron beam irradiation [17-19] are examples to the methods used to affect the molecular structure of certain polymers, including LDPE, and hence study its influence on the properties of these polymers. Photo-oxidation using UV irradiation has also gained wide interest in literature [20, 21]. Studying the rheological behavior of LDPE at temperatures exceeding their melting temperature and under UV irradiation was the goal of Marek and Verney [22] where they concluded that LDPE has shown less chain-cession compared to HDPE and PP. On the other hand, UV irradiation of LDPE/montmorillonite nano-composites did not gain similar attentiveness in literature. Sánchez-Valdés *et. al.* [23] studied the effect of photo-oxidation on two groups of LDPE/ clay nano-composites where they concluded that clay has enhanced the degradation rate of the nano-composites compared to the raw PE material.

In this study we irradiated an arbitrary selected composition of LDPE/MMT composite using short wavelength UV source. UV irradiation was conducted at two different isothermal crystallization temperatures in order to investigate its effect on the molecular and crystalline structure of these composites.

## 2. Experimental procedure:

### 2.1. Materials

The raw material of low density polyethylene (LDPE) used in this study is a commercial grade produced by SABIC (HP4023W) company. The melt flow rate of this product is 4.0 g/10min. according to ASTM D1238. The nano-clay nanomer 1.44P is a montmorillonite clay surface modified with 35-45 wt. % dimethyl dialkyl (C14-C18) amine and is a product of Sigma Aldrich. The Maleic Anhydride grafted polyethylene (MA-g-PE) is used as a compatibilizer and is also a product of Sigma Aldrich.

### 2.2 Sample preparation:

A mixture of 93 wt. % of LDPE, 3 wt. % of MA-g-PE and 4 wt. % of nano-clay was prepared by melt mixing it using Dynisco laboratory mixer. The barrel temperature was set at 140°C, while the orifice temperature was set at 130°C. The homogeneous compound was quenched in water at room temperature. The compound was then slightly pressed at 140°C using Carver hot press to form homogeneous films of a thickness of about 0.1 mm.

Samples were divided into two main groups based on the method of UV treatment. A short UV wavelength of 254 nm at a distance of 13 cm was used for all samples as summarized in table 1.

Table 1 List of the nomenclature of the samples used.

Composite's symbol	UV treatment method	$T_c$ (°C)
A100	Samples were exposed to UV radiation for 5 hours during the isothermal crystallization process.	100
A104		104
D100	Samples were not exposed to any UV radiation.	100
D104		104

Using Linkam T95-HS hot stage, the heating profile used to crystallize the samples was as follow: melting at 130°C for 10 minutes to remove any thermal history; then rapidly cooling down to an arbitrary selected crystallization temperature of  $T_c = 100^\circ\text{C}$  or  $104^\circ\text{C}$ ; annealing for 5 hours to allow sufficient time for complete crystallization.

### 2.3 Testing methods:

Wide angle x-ray diffraction patterns were obtained by using BrukerD8 advance X-ray diffractometer with Cu  $K_\alpha$  radiation of wavelength  $\lambda = 0.154$  nm, a running voltage of 40.0 (kV) and a current of 40.0 (mA).

DSC endotherms were taken using Perkin Elmer DSC 8000. All samples were heated at the rate of 10°C/min, then cooled down to room temperature at the same rate.

FTIR spectra were taken for all samples using Nicolet iS5 FTIR spectrometer in the mid-IR range ( $400 - 4000$   $\text{cm}^{-1}$ ) at a resolution of  $2$   $\text{cm}^{-1}$ .

### 3. Data and results:

The single broad endotherm peak, appears in the melting behavior of raw LDPE material see Fig. 1, indicates a relatively wide molecular weight distribution with a melting peak of 109.4°C. Two second order transitions at around 59°C and 73°C are observed. The two second order transitions are believed to be due to the presence of the slip and anti-block additives that were added to the raw material, as specified in the data sheet of LDPE raw material.

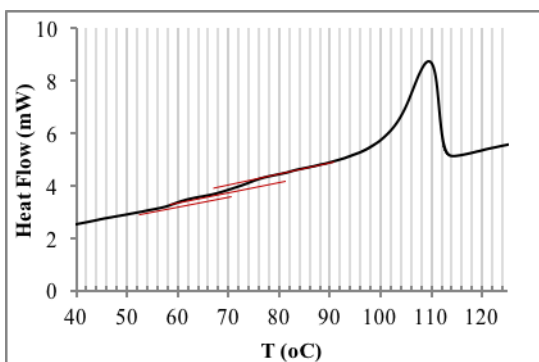


Figure 1 DSC endotherm of raw LDPE

The melting behavior of sample D is shown in Fig. 2. As can be observed, its melting behavior differs significantly with changing the isothermal crystallization temperature. Three distinct peaks have appeared for both crystallization temperatures. All samples show three distinct peaks. At lower temperature, in the range of 96.0°C, a broad melting peak with small heat flow appears; while a peak with smaller FWHM and higher heat flow values appears in the range of 106.0°C. At around 109.5°C a third peak that is sharper and has larger heat flow values appears. This melting point coincides with that of the raw material, which suggests that at this temperature similar crystalline phases have melted. The absence of the multi-peak behavior of the raw material (Fig. 1) suggests that the addition of MMT and PE-g-MA is the reason behind this action.

The multi-peak behavior in DSC thermographs could be attributed to either the presence of different crystalline structures or to the different molecular weight population. In this work it is believed that both interpretations are valid. The small and broad peak at lower temperature is believed to be due to the melting of crystals that

were formed by relatively low molecular weight chains [24]. These chains start to segregate producing some form of organized entities during the cooling process from melting to the crystallization temperature [25].

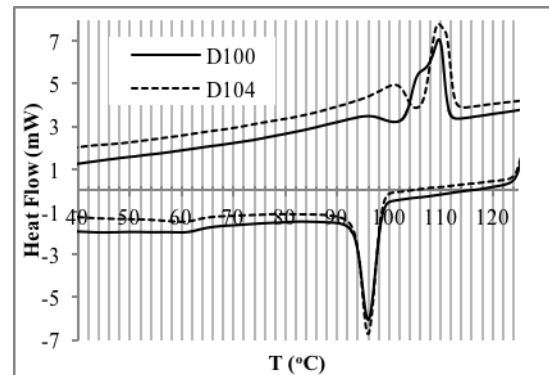


Figure 2 DSC thermographs of sample D crystallized at 100 and 104°C.

The other two larger peaks are believed to be due to the formation of two different crystalline phases: the monoclinic and orthorhombic phases [26]. As will be discussed later, peak 2 is believed to refer to the melting of the monoclinic phase while peak 3 represents the melting of the orthorhombic phase. Similar argument can be suggested for sample A 100 as illustrated in Fig. 3.

On the other hand, although samples A and D that were crystallized at 104°C have shown similar multi-peak behavior, the positions of these peaks have changed towards larger temperatures. Peak 1 has shifted to the range of 100°C, which suggests that the small entities crystallized during the cooling process managed to grow more, forming extended crystalline entities and hence larger melting temperatures.

Peak 2 has shifted 4-5°C towards larger temperatures to about 111°C. It is believed that annealing the composite at lower super-cooling temperatures allowed the chains of the monoclinic crystals to extend more due to the larger chain mobility at higher temperatures. Peak 3 however, did not change its position. Apparently orthorhombic crystals are very stable and did not show any respond to the change in crystallization temperature. This observation contradicts with what is reported in literature where larger crystallization temperatures yielded larger melting points [27-29]. This contradiction could be

justified by assuming that the orthorhombic crystals are formed by the longer molecular chains. It is possible that the branches of these molecules hinder any additional growth of the orthorhombic crystals.

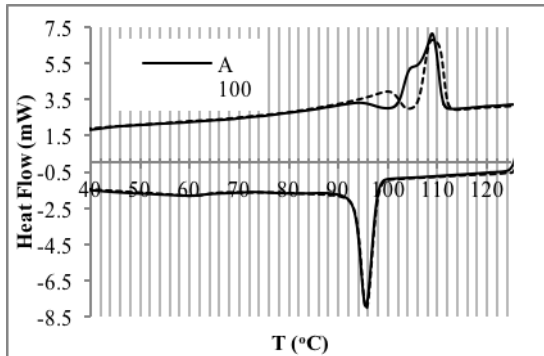


Figure 3 DSC endotherms and exotherms of sample A crystallized at 100 and 104 °C.

Crystals formed in the monoclinic phase, however, have the ability to include these branches in the crystalline phase which, consequently, allow for the extension of chains in the crystalline phase, and hence requires larger heat energy to melt it.

By comparing the melting temperatures of samples A and D, listed in Table 2, it can be noticed that sample D is more thermally stable than sample A. This can be noticed from the larger values of the melting and crystallization peaks of sample D100 compared to A100 and D104 compared to A104. This behavior is expected since sample D was not exposed to UV radiation hence no chain-scissions have occurred.

The UV exposure of sample A during the crystallization process is responsible for reducing its thermal stability. It is suggested that during the crystallization process free radicals are generated. Such free radicals are responsible for chain-scission especially for small molecular chains as suggested by the temperature difference of peak 1. Peak 3, in general, has shown less respond to UV exposure. In conclusion, the exposing method used for sample A has significant effect only on both monoclinic phase and the low molecular weight population. Further studies are required to understand the time effect of UV exposure on the thermal stability of these phases.

Table 2 List of the peak positions obtained from DSC thermographs.

Composite's symbol	$T_m(^{\circ}\text{C})$ peak 1	$T_m(^{\circ}\text{C})$ peak 2	$T_m(^{\circ}\text{C})$ peak 3	$T_c(^{\circ}\text{C})$ peak
Raw material	--	--	109.38	94.55
A100	92.94	104.54	109.39	95.73
A104	99.71	110.32	108.86	95.51
D100	95.05	105.51	109.71	96.16
D104	101.00	110.96	109.70	96.12

XRD results shown in Fig.4 and Fig. 5 coincide with what was suggested by DSC. The two (110) and (200) orthorhombic peaks appear at angles  $2\theta \approx 21.7^{\circ}$  and  $24.0^{\circ}$  respectively, while the monoclinic (010) appears at  $2\theta \approx 19.6^{\circ}$  [30]. The appearance of both crystalline phases could not be referred to the addition of MMT or MA since these phases appear in the diffraction of raw material too (Fig. 4). However, the two peaks formed at lower scattering angles  $2\theta \approx 2.5^{\circ}$  and  $4.9^{\circ}$  are referred to the addition of MMT clay in which intercalated nano-composites are formed [31]. Comparing XRD results with DSC thermal behavior we can conclude that the endotherm peaks formed at larger temperatures ( $\sim 109.5^{\circ}\text{C}$ ) in Figs. 2 and 3 are due to the melting of the orthorhombic crystals while those formed at temperature near  $104^{\circ}\text{C}$  represent the melting of the monoclinic crystals.

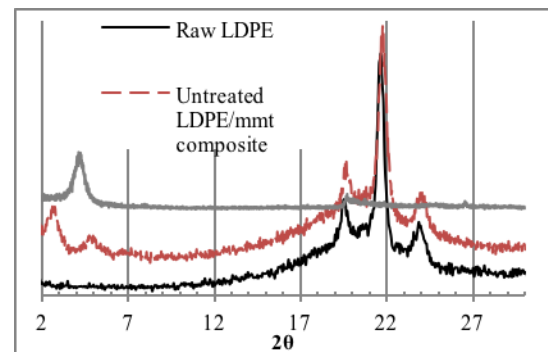


Figure 4 X-ray diffractions of raw LDPE, LDPE composite without treatment and clay.

XRD spectra of samples A100 and D100 shown in Fig. 5 did not show any change in the type or size of crystals formed. This could be concluded from the absence of any new peaks or any shift in the peak positions. The fact that the  $d_{001}$  and  $d_{002}$  spacing of the silicate layers is larger for sample D, as listed in Table 3, induces that UV exposure jeopardizes the intercalation process. Free radicals are possibly interacting with the

anions and cations in between the layered silicates causing its intermolecular spacing to decrease.

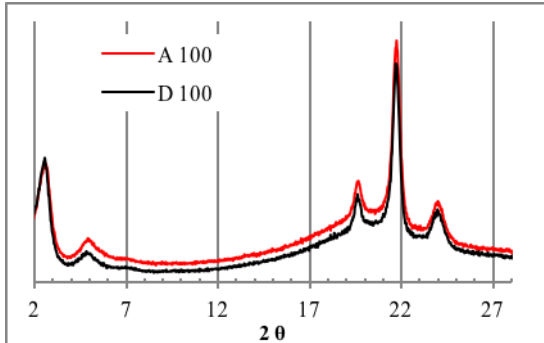


Figure 5 X-ray diffractions of samples crystallized at 100 °C

Table 3 List of *d* spacings of the two peaks generated due to the existence of MMT

Sample	2θ	<i>d</i> <sub>001</sub> (Å)	2θ	<i>d</i> <sub>002</sub> (Å)
A100	2.53	34.852	4.93	17.923
A104	2.48	35.595	5.00	17.674
D100	2.49	35.512	4.86	18.164
D104	2.47	35.736	4.78	18.480

Another possible interpretation to these results is that the molecules of maleic anhydride are largely affected by free radicals causing some chain-cission to occur. This will eventually affect the compatibility between the clay and polymer hence causing some of LDPE chains to be expelled from in between the layered silicates. This observation is in agreement with the depression of the non-isothermal crystallization temperature listed in Table 2.

FTIR spectra shown in Fig. 6 represent those of the three reference materials: MMT, raw LDPE and the untreated LDPE/MMT composite. The spectra were taken for a full range of 400-4000 cm<sup>-1</sup>, however, our focus will be on the limited range of 700-1500 cm<sup>-1</sup>. The importance of this range comes from the fact that it includes both the rocking CH<sub>2</sub> mode (700-740 cm<sup>-1</sup>) and the bending CH<sub>2</sub> mode (700-740 cm<sup>-1</sup>).

The rocking CH<sub>2</sub> mode of samples A100 and D100 are illustrated in Fig. 7, where the left side peaks at 719 cm<sup>-1</sup> represent the ordered chains of the monoclinic phase and the right side peaks at 730 cm<sup>-1</sup> refer to the orthorhombic crystalline structure [32]. The relative intensities of these two peaks are comparable for A100, while D100 shows a dominating monoclinic phase. At an isothermal crystallization temperature of *T*<sub>c</sub> =

104°C (Fig. 8) more rocking mode chains are formed in the monoclinic phase. The equivalent intensities of sample A100 (Fig. 7) could be referred to the UV exposure of the sample, where more of the rocking mode chains are crystallizing in the orthorhombic phase.

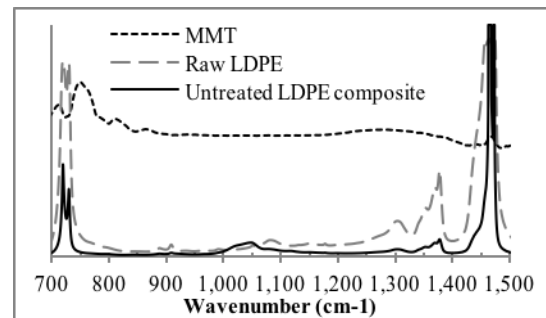


Figure 6 FTIR spectra of rawLDPE, MMT and an untreated composite

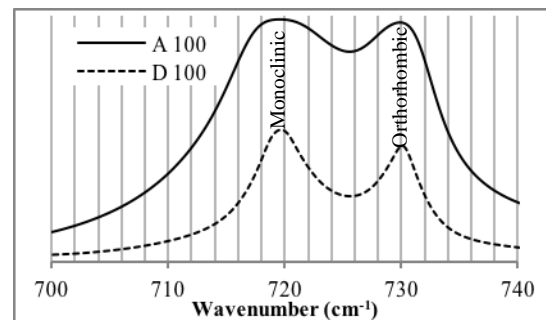


Figure 7 FTIR spectra of A100 and D100 in the rocking mode

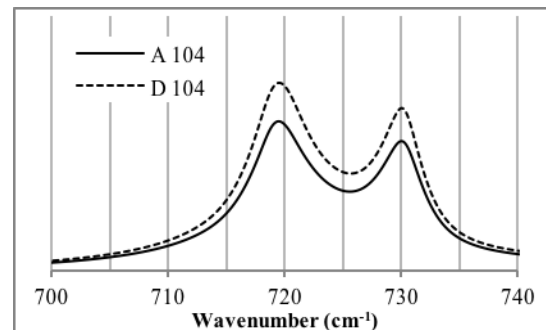


Figure 8 FTIR spectra of A104 and D104 in the rocking mode

The absorption spectra of the bending mode of methylene groups are illustrated in Figs. 9 and 10. Bands in the (1461-1463 cm<sup>-1</sup>) region represent the absorption of the all *trans* orthorhombic chains, while the (1466-1467 cm<sup>-1</sup>) region represents the all *trans* amorphous molecules. The 1472 cm<sup>-1</sup>, however, is believed to represent the dominating phase of monoclinic crystals. The



broad spectrum of A100 in Fig. 9 is due to the large thickness of the sample used hence cannot be included in this discussion.

Generally, the relative intensity  $I_{\text{Mon.}}/I_{\text{Orth.}}$  of the bending mode is larger than that of the rocking mode for all samples studied. This explains the dependency of the melting temperature of monoclinic phase on the isothermal crystallization temperature and UV exposure.

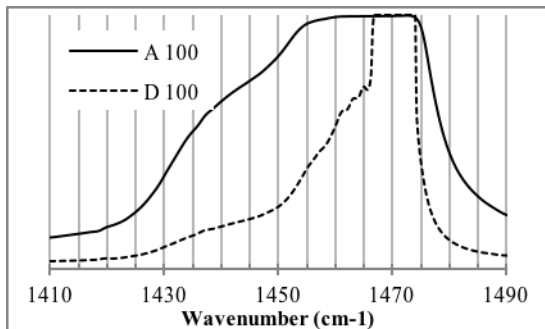


Figure 9 FTIR spectra of A100 and D100 in the bending mode

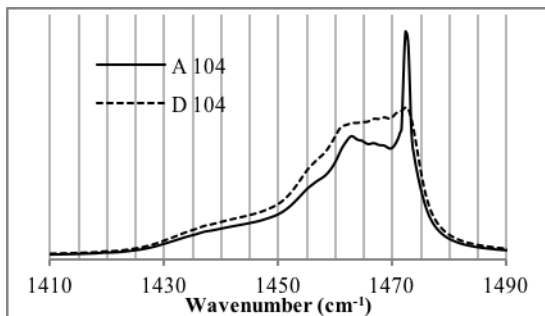


Figure 10 FTIR spectra of A104 and D104 in the bending mode

An exception to this discussion could be made for sample D104, where its  $I_{\text{Mon.}}/I_{\text{Orth.}}$  is close to unity. The less domination of the monoclinic phase and the obvious presence of the amorphous phase, in addition to the fact that this sample has the largest  $d_{001}$  silicate spacing as listed in Table 1, suggest that an additional monoclinic chains might have been intercalated in between the layered silicates hence its bending vibration was hindered due to the smaller degree of freedom. Accordingly, it can be suggested that for better intercalation process samples should be isothermally crystallized at lower super cooling temperatures. In order to confirm this assumption further studies are required.

#### 4. Conclusion:

In this study we tried to study the effect of both isothermal crystallization temperature and UV exposure on the behavior of LDPE/MMT nano-composites and hence their effect on the properties of these composites. By varying the two parameters we attempted to obtain the optimum conditions for the intercalation process; and consequently optimize the mechanical properties of these nano-composites.

XRD results showed that the nano-composites compose of two stable crystalline structures, orthorhombic and monoclinic, in addition to a third phase of crystalline small chain entities. UV exposure has less effect on the thermal stability of LDPE/MMT nano-composites compared to the effect of isothermal crystallization temperatures. The monoclinic crystalline structure has responded more effectually to the change of crystallization conditions compared to the orthorhombic structure.

Chains growing in the monoclinic phase allow the small branches of LDPE to be included in the crystalline phase hence extending the molecular chains of the crystalline phase. In contrast, orthorhombic crystals showed no sign of chain extension and, consequently, no sign of branch inclusion.

Intercalation process was affected by the method of UV exposure. UV radiation jeopardized the intercalation process. However, a sign of better intercalation is observed at larger isothermal crystallization temperature.

#### Acknowledgments

This work has been funded by the deanship of scientific research at Majmaah University under grant number 16. The help and support of the dean of scientific research and the head of Physics Department Dr. Thamer Alharbi is greatly appreciable. All measurements were done in our Materials Science Research Lab.

#### References

- [1] Qin, H., Zhang, S., Liu, H., Xie, S., Yang, M., Shen, D., 2005. Photo-oxidative degradation of

- polypropylene/montmorillonite nanocomposites. *Polymer* 46(9), pp 3149–3156.
- [2] Manias, E., Touny, A., Wu, L., Strawhecker, K., Lu, B., Chung, C., 2001. Polypropylene/Montmorillonite Nanocomposites. Review of the Synthetic Routes and Materials Properties. *Chemistry of Material* 13, pp 3516-3523.
- [3] Gerald, S., 1990. Polymers with enhanced photodegradability. *Journal of Photochemistry and Photobiology A: Chemistry* 51(1), pp 73–79.
- [4] <http://www.plasticseurope.org/plastics-industry/market-and-economics.aspx>
- [5] Li, J., Shanks, R.A. and Long, Y., 2001. Isothermal crystallization and spherulite structure of partially miscible polypropylene–linear low-density polyethylene blends. *Journal of applied polymer science* 82(3), pp.628-639.
- [6] Martuscelli, E., Pracella, M., Volpe, G.D. and Greco, P., 1984. Morphology, crystallization, and thermal behaviour of isotactic polypropylene/low density polyethylene blends. *Die Makromolekulare Chemie* 185(5), pp.1041-1061.
- [7] Schouterden, P., Groeninckx, G., Van der Heijden, B. and Jansen, F., 1987. Fractionation and thermal behaviour of linear low density polyethylene. *Polymer* 28(12), pp.2099-2104.
- [8] Janigová, I., Chodák, I. and Chorváth, I., 1992. The influence of crosslinking on isothermal crystallization of LDPE filled with silica. *European polymer journal* 28(12), pp.1547-1552.
- [9] Grady, B.P., Genetti, W.B., Lamirand, R.J. and Shah, M., 2001. An investigation of heat transfer effects in isothermal crystallization studies of low-density polyethylene. *Polymer Engineering & Science* 41(5), pp.820-829.
- [10] Hargis, M.J. and Grady, B.P., 2006. Effect of sample size on isothermal crystallization measurements performed in a differential scanning calorimeter: A method to determine avrami parameters without sample thickness effects. *Thermochimica acta* 443(2), pp.147-158.
- [11] Dhillon, R., K., Singh, P., Gupta, S., K., Singh, S., Kumar, R., 2013. Study of high energy (MeV)  $N^{6+}$  ion and gamma radiation induced modifications in low density polyethylene (LDPE) polymer. *Nuclear Instruments and Methods in Physics Research Section B: Beam Interactions with Materials and Atoms* 301, pp 12–16.
- [12] Singh, R., Samra, K., S., Kumar, R., Singh, L., 2008. Proton (3MeV) and copper (120MeV) ion irradiation effects in low-density polyethylene (LDPE). *Radiation Physics and Chemistry* 77(1), pp 53–57.
- [13] Vinodh, Kumar, S., Ghadei, B., Krishna, J., B., M., Bhattacharya, S., C., Saha, A., 2009. High-energy  $C^{+}$  ion-irradiated low-density polyethylene (LDPE): Spectroscopic and morphological investigation. *Radiation Physics and Chemistry* 78(5), pp 351–355.
- [14] Zhang, J., Rahman, A., Z., M., S., Li, Y., Yang, J., Wu, Y., Yuan, D., Wang, B., 2015. Radiation induced modifications on structural and luminescence properties of LDPE– $Na_2SO_4:Sm^{3+}$  composites by  $\gamma$ -ray. *Optical Materials* 42, pp 251–255.
- [15] Moez, A., A., Aly, S., S., Elshaer, Y., H., 2012. Effect of gamma radiation on low density polyethylene (LDPE) films: optical, dielectric and FTIR studies. *Spectrochimica Acta. Part A, Molecular and Biomolecular Spectroscopy* 93, pp 203–207.
- [16] Alvarez, V., A., Perez, C., J., 2013. Gamma irradiated LDPE in presence of oxygen. Part I. Non-isothermal crystallization. *Thermochimica Acta* 570, pp 64–73.
- [17] Han, J., Castell-Perez, M., E., Moreira, R., G., 2007. The influence of electron beam irradiation of antimicrobial-coated LDPE/polyamide films on antimicrobial activity and film properties. *LWT - Food Science and Technology* 40(9), pp 1545–1554.
- [18] Sabet, M., Hassan, A., Ratnam, C., T., 2012. Electron beam irradiation of low density polyethylene/ethylene vinyl acetate filled with metal hydroxides for wire and cable applications. *Polymer Degradation and Stability* 97(8), pp 1432–1437.
- [19] Soltani, Z., Ziaie, F., Ghaffari, M., Afarideh, H., Ehsani, M., 2013. Mechanical and thermal properties and morphological studies of 10MeV electron beam irradiated LDPE/hydroxyapatite nano-composite. *Radiation Physics and Chemistry* 83, pp 79–85.
- [20] Dintcheva, N., T., Alessi, S., Arrigo, R., Przybytniak, G., Spadaro, G., 2012. Influence of the e-beam irradiation and photo-oxidation aging on the structure and properties of LDPE-OMMT nanocomposite films. *Radiation Physics and Chemistry* 81(4), pp 432–436.
- [21] Giesse, R., De Paoli, M.-A., 1988. Surface and bulk oxidation of low-density polyethylene under UV-irradiation. *Polymer Degradation and Stability* 21(2), pp 181–187.
- [22] Marek, A., A., Verney, V., 2015. Rheological behavior of polyolefins during UV irradiation at high temperature as a coupled degradative process. *European Polymer Journal* 72, pp 1–11.
- [23] Sánchez-Valdés, S., Martínez, Colunga, J., G., López-Quintanilla, M., L., Yañez, Flores, I., García-Salazar, M., L., González, Cantu, C., 2008. Preparation and UV weathering of polyethylene nanocomposites. *Polymer Bulletin* 60(6), pp 829–836.
- [24] Maxwell, A., S., A., P., Unwin, I., M., Ward, M.I., Abo El Maaty, M., M., Shahin, R., H., Olley, D., C., Bassett, 1997. The effect of molecular weight on the deformation behaviour of pressure annealed polyethylene. *Journal of materials science* 32(3), pp 567-574.
- [25] Kim, M., H., Phillips, P., J., 1998. Nonisothermal melting and crystallization studies of homogeneous ethylene/ $\alpha$ -olefin random copolymers. *Journal of applied polymer science* 70(10), pp 1893-1905.
- [26] Vanden, Eynde, S., Sanjay, Rastogi, V., B., F., Mathot, Harry, Reynaers, 2000. Ethylene-1-octene copolymers at elevated pressure-temperature. 1. Order-disorder transition. *Macromolecules* 33(26), pp 9696-9704.
- [27] Shi, X., Jin, J., Chen, S. and Zhang, J., 2009. Multiple melting and partial miscibility of ethylene-vinyl acetate copolymer/low density polyethylene blends. *Journal of applied polymer science* 113(5), pp.2863-2871.
- [28] Wang, C., Chu, M.C., Lin, T.L., Lai, S.M., Shih, H.H. and Yang, J.C., 2001. Microstructures of a highly short-chain branched polyethylene. *Polymer* 42(4), pp.1733-1741.
- [29] Dimeska, A. and Phillips, P.J., 2006. High pressure crystallization of random propylene–ethylene copolymers:  $\alpha$ - $\gamma$  Phase diagram. *Polymer* 47(15), pp.5445-5456.
- [30] Vanden, Eynde, S., Rastogi, S., Mathot, V., B., F., Reynaers, H., 2000. Ethylene-1-octene copolymers at elevated pressure-temperature. 1. Order-disorder transition. *Macromolecules* 33(26), pp 9696-9704.
- [31] Liu, S.-P., Tu, L.-C., 2011. Studies on mechanical properties of dispersing intercalated silane montmorillonite in low density polyethylene matrix. *International Communications in Heat and Mass Transfer* 38(7), pp 879–886.
- [32] Pilar, T., Julio, G., Rafael, S., Mario, H., Nuria, G., 2009. Evidence of a monoclinic-like amorphous phase in composites of LDPE with spherical, fibrous and laminar nanofillers as studied by infrared spectroscopy. *European Polymer Journal* 45, pp 30–39.